Subaru Near Infrared Coronagraphic Images of T Tauri *

Satoshi Mayama,[1,2] Motohide Tamura,[3] Masahiko Hayashi,[1] Yoichi Itoh,[4] Misato Fukagawa,[5]
Hiroshi Suto,[3] Miki Ishii,[1] Koji Murakawa,[6] Yumiko Oasa,[4] Saeko S. Hayashi,[1] Takuya Yamashita,[1]
Junichi Morino,[3] Shin Oya,[1] Takahiro Naoi,[7] Tae-Soo Pyo,[1] Takayuki Nishikawa,[1,2]
Tomoyuki Kudo,[2,3] Tomonori Usuda,[1] Hiroyasu Ando,[3] Shoken M. Miyama,[3] and Norio Kaifu[3]

[1]*Subaru Telescope, National Astronomical Observatory of Japan, 650 North A'ohoku Place, Hilo, HI 96720, USA*
mayamast@subaru.naoj.org

[2]*School of Mathematical and Physical Science, The Graduate University for Advanced Studies, 2-21-1 Osawa, Mitaka, Tokyo 181-8588*

[3]*Optical and Infrared Astronomy Division, National Astronomical Observatory of Japan, 2-21-1 Osawa, Mitaka, Tokyo 181-8588*

[4]*Graduate School of Science and Technology, Kobe University, 1-1 Rokkodai, Nada-ku, Kobe 657-8501*

[5]*Division of Particle and Astrophysical Sciences, Nagoya University, Furo-cho, Chikusa-ku, Nagoya 464-8602*

[6]*Astronomisch Onderzoek in Netherlands (ASTRON), PO Box 2, 7990 AA, Dwingeloo, The Netherlands*

[7]*Institute of Space and Astronautical Science, Japan Aerospace Exploration Agency,*
3-1-1 Yoshinodai, Sagamihara, Kanagawa 229-8510

Abstract

High angular resolution near-infrared (*JHK*) adaptive optics images of T Tau were obtained with the infrared camera Coronagraphic Imager with Adaptive Optics (CIAO) mounted on the 8.2 m Subaru Telescope in 2002 and 2004. The images resolve a complex circumstellar structure around a multiple system. We resolved T Tau Sa and Sb as well as T Tau N and S. The estimated orbit of T Tau Sb indicates that it is probably bound to T Tau Sa. The *K* band flux of T Tau S decreased by ~ 1.7 Jy in 2002 November compared with that in 2001 mainly because T Tau Sa became fainter. The arc-like ridge detected in our near-infrared images is consistent with what is seen at visible wavelengths, supporting the interpretation in previous studies that the arc is part of the cavity wall seen relatively pole-on. Halo emission is detected out to $\sim 2''$ from T Tau N. This may be light scattered off the common envelope surrounding the T Tauri multiple system.

Key words: stars: individual (T Tauri) — stars: pre-main sequence — ISM: reflection nebula

1. Introduction

T Tau has long been identified as one of the brightest low-mass pre–main-sequence objects and, as such, has been considered as a prototype for the T Tauri class of objects (Joy 1945). Its notable prototypical properties are as follows: (1) A significant infrared continuum excess, thought to be related to the presence of an accretion disk around this million-year-old object (Bertout et al. 1988); (2) A bright nebulosity caused by photons scattering off the inner wall of a cavity emptied by a strong polar outflow from T Tau (Stapelfeldt et al. 1998); (3) A substantial circumstellar disk resolved by interferometric imaging at radio wavelengths (Akeson et al. 1998); (4) A modest interstellar extinction ($A_V \sim 1.5$ mag; Ghez et al. 1991).

There are, however, several atypical features. Dyck, Simon, and Zuckerman (1982) discovered T Tau S, an infrared companion of T Tau (now called T Tau N) by means of one-dimensional near-infrared speckle scanning. T Tau S is located $0''.7$ south of the primary T Tau N (Dyck et al. 1982), or 100 AU away in the projected scale, if we assume a distance of 140 pc to the Taurus dark cloud complex (Elias 1978). T Tau S has a spectral energy distribution that peaks around 3μm, making it significantly redder than a normal T Tauri star (Ghez et al.

1991). It dominates the total flux from the T Tau system at wavelengths longer than 2μm, which makes its bolometric luminosity about twice as large as that of T Tau N (Stapelfeldt et al. 1998). Near- to mid-infrared monitoring observations have revealed that T Tau S is variable, up to 2 mag over a few months (Ghez et al. 1991). Its near-infrared spectrum is featureless around 2μm at a resolution of $R \sim 760$, except for a strong Brγ emission line and a much weaker H$_2$ $v = 1$–0 S(1) line (Beck et al. 2001). Koresko, Herbst, and Leinert (1997) suggested from these unique properties of T Tau S that it is (a) an embedded intermediate- to high-mass protostar, (b) a planetary object embedded in a disk around T Tau N, or (c) a strongly accreting FU Ori-like object, although none of these explain all the observational data.

Koresko (2000) further found by speckle holography observations that T Tau S, itself, is a binary system of T Tau Sa and Sb. The binary has a separation of $\sim 0''.05$ or ~ 7 AU. Köhler, Kasper, and Herbst (2000) discovered that the binary separation and position angle vary with time, suggesting that T Tau Sa and Sb are gravitationally bound with an orbital period of 10–20 yr. A recently calculated orbit of the T Tau Sa and Sb pair, based upon 17 astrometric measurements, showed that the orbit has a period of 33 yr and a semimajor axis of $0''.104$ (14.6 AU) (Tamazian 2004). The sum of the masses of T Tau Sa and Sb was found to be $(2.82 \pm 0.74) M_\odot$ with 2.2 $M_\odot$ for T Tau Sa, which was the first direct estimate of the mass for Sa.

---

* Based on data collected at Subaru Telescope, which is operated by the National Astronomical Observatory of Japan.

Very Large Array observations resolved the T Tau system into two compact components at 2 cm, one coincident with T Tau N and a brighter one close to T Tau S (Schwartz et al. 1986). The southern radio component, unresolved in VLBI images (diameter < 0.5 mas; Smith et al. 2003), was until recently identified as T Tau Sb because it had a proper motion consistent with the orbital motion around T Tau Sa (Johnson et al. 2003; Loinard et al. 2003), which was not detected in the radio data. The radio source, however, has been found to show an apparently ejected trajectory (Loinard et al. 2003), and is now called T Tau Sc (Furlan et al. 2003), not necessarily the same as T Tau Sb.

In order to gain a better understanding of the nature of the T Tau system and its circum-multiple structure, we conducted high-resolution coronagraphic imaging observations in the near-infrared. Coronagraphy is a useful technique to obtain high-contrast images of faint circumstellar matter and companions around a bright central object, such as T Tau ($K \sim 5.53$ mag; Beck et al. 2004). Robberto et al. (1995), Nakajima and Golimowski (1995), and Weinstraub et al. (1992) previously reported optical and infrared coronagraphic observations of T Tau. These observations were, however, made with relatively large (a few arcsec) occulting masks. In this paper, we present the adaptive optics (AO, Takami et al. 2004) coronagraphic images of T Tau obtained with the Subaru Telescope using a mask size of $0''5$–$0''6$ in diameter. Observations and data-reduction procedures are described in sections 2 and 3, respectively. The results and discussions are presented in section 4. Section 5 summarizes the conclusions.

2. Observation

Observations were carried out on 2002 November 20 with the Coronagraphic Imager with Adaptive Optics (CIAO, Tamura et al. 2000) on the 8.2 m Subaru Telescope. CIAO has occulting masks at the focal plane and circular Lyot stops at the pupil plane, both cooled cryogenically. The occulting masks are made of chrome on a sapphire substrate and have a transmittance of $\sim 2\%$, which enables us to measure the exact position of a masked object. Position adjustments to the center of a mask during observations were performed to obtain long-exposure data without any displacement in position. We used an occulting mask with a diameter of $0''5$ and a Lyot stop with 80% of the pupil diameter with the medium-resolution imaging mode of CIAO. While a low-order AO coronagraph does not effectively suppress the halo of PSF, it allows exposure time longer than that of an observation without a coronagraph. This enables us to reduce the effect of any read-out noise, making more efficient use of the observation time. Another incidental benefit of coronagraphy is to reduce optics-induced scattering after the focal plane mask. The pixel scale and the position angle of the 1024×1024 InSb array (ALADDIN II) were measured by observations of the Trapezium (Simon et al. 1999) with the same optical configurations for the T Tau observations, and were $0''0213 \pm 0''0003$ pixel^{-1} and $5°.7 \pm 0°.8$, respectively. The field of view was $22'' \times 22''$. The observations were carried out in the J, H, and K bands centered at 1.25, 1.65, and 2.2 μm, respectively. We used T Tau N as an adaptive optics guide star (AO, Takami et al. 2004). The sky was clear and

photometric, although the seeing was variable.

We obtained 18, 48, and 48 frames for T Tau with $2 \, \mathrm{s} \times$ 5 co-adds, $2 \, \mathrm{s} \times 5$ co-adds, and $1 \, \mathrm{s} \times 10$ co-adds for the J, H, and K bands, respectively. We imaged SAO 75661 (J band), HD 283567 (H band), and HD 286794 (K band) for PSF reference before and after the T Tau observations with the same configurations. We selected different PSF reference stars for different bands in order to obtain a reference-star magnitude similar to that of T Tau at any observing wavelength. This was necessary because the AO corrected PSF varies with the AO reference-star magnitude. We obtained 4, 16, and 24 frames with $10 \, \mathrm{s} \times 6$ co-adds, $10 \, \mathrm{s} \times 6$ co-adds and $5 \, \mathrm{s} \times 2$ co-adds for the J, H, and K band reference stars, respectively. The photometric standard star FS4 (UKIRT catalog)[1] was imaged without an occulting mask in the beginning of the observations. Sky frames were taken after the observations of T Tau. Dome flats and dark frames were taken at the end of the night.

We made additional K band observations on 2004 November 23 with CIAO in order to measure the position of T Tau Sb. The average natural seeing was $1''0$, and an occulting mask with a diameter of $0''6$ was used with AO. The pixel scale and position angle of the detector, measured as in the first run, were $(0''0213 \pm 0''0001)$ pixel^{-1} and $1°.68 \pm 0°.27$. We obtained 20, 6, and 10 frames for T Tau with $0.5 \, \mathrm{s} \times 1$ co-add, $0.5 \, \mathrm{s} \times$ 10 co-adds, and $1 \, \mathrm{s} \times 10$ co-adds, respectively. Neither PSF reference stars nor photometric standard star were observed. Dark frames were taken at the end of the night. Dome flats were taken 1 day before the observations.

3. Data Reduction

The Image Reduction and Analysis Facility (IRAF) software was used for all data reduction. A dark frame was subtracted from each object frame, which was then divided by the dome-flat. Hot and bad pixels were removed and the sky was subtracted. The same reduction sequence was applied for the reference stars.

Although we carried out observations with the AO, the peak-intensity position of the PSF changed slightly during the observations. This was mainly caused by the difference in atmospheric dispersion between the infrared wavelength at which the images were taken and the optical wavelength at which the wave front was measured. We measured the peak position of the reference star PSF with the IMEXAMINE task in IRAF and shifted the images. Since Subaru is an alt-azimuth telescope, and we used an instrument rotator; the position angle of the spider pattern changed with time. The reference star frames were accordingly rotated so that the position angle of the spider would match that of each object frame. We subtracted the reference star PSFs from the object frames in order to visualize the faint structure around the primary T Tau N by eliminating its halo pattern. However, the PSF, especially its width, varied with time as the seeing changed. We thus sorted out all of the object and reference star frames into 3 groups by the widths (FWHMs) of their PSFs. The FWHM boundaries of each categorized group in each band are as follows. The 3 groups in the J band are FWHM $> 0''15$,
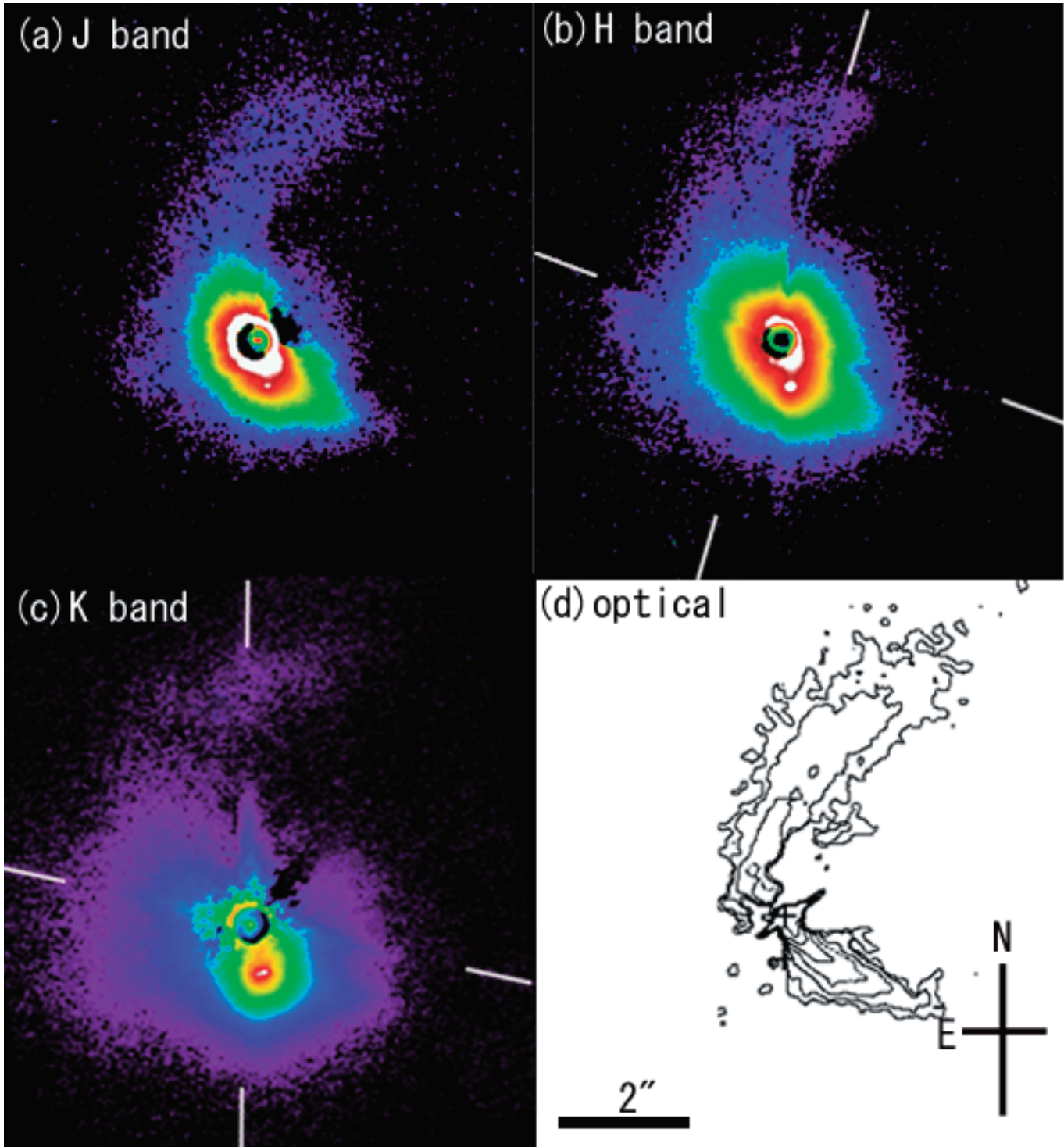
---

[1] ⟨http://www.jach.hawaii.edu/UKIRT/⟩.

Fig. 1. (a) J, (b) H, and (c) K band CIAO images and (d) optical HST contour map (Stapelfeldt et al. 1998, reproduced by permission of the AAS) of T Tau. PSFs of the central star were subtracted. The directions of the spider patterns are indicated by white lines in the H and K band images. The field of view is $8'' \times 9''$ in the all four images. North is up and east toward the left. In the HST contour map, locations of the primary star and infrared companion are indicated by the two crosses. The dotted contour level is $15\,\mathrm{mag\,arcsec}^{-2}$, and contours are separated by $1\,\mathrm{mag\,arcsec}^{-2}$.

$0''\!.15 > \mathrm{FWHM} > 0''\!.1$, and $\mathrm{FWHM} < 0''\!.1$. The 3 groups in the H band are $\mathrm{FWHM} > 0''\!.1$, $0''\!.1 > \mathrm{FWHM} > 0''\!.08$, and $\mathrm{FWHM} < 0''\!.08$. The 3 groups in the K band are $\mathrm{FWHM} > 0''\!.09$, $0''\!.09 > \mathrm{FWHM} > 0''\!.07$, and $\mathrm{FWHM} < 0''\!.07$. In each group the reference star PSFs were averaged and the resultant PSF was scaled so that the average count at its halo (radius $> 0''\!.4$) matched that of each object frame in the same group. The scaled reference star PSFs were then subtracted

from the corresponding object frames. For the 18 J band object frames, 14 frames had PSFs that did not match well with the reference star PSF and were rejected. We combined all the PSF subtracted frames of each band to produce the final image. The calibrated images are available on request.

The J, H, and K band coronagraphic images of T Tau multiple system obtained in 2002 are presented in figure 1 together with an HST optical image (Stapelfeldt et al. 1988). The total integration times for the 2002 November images were 40 s, 480 s, and 480 s for the J, H, and K bands, respectively, after frames with poor AO correction were rejected. The total integration time for the 2004 November K image was 140 s after frames with poor AO correction were rejected. The final images had a flux uncertainty of up to 20% because of the differences in size and shape of PSF between the object and reference stars. The PSFs of the final images have sizes of $0{.}''1$, $0{.}''08$, and $0{.}''07$ (FWHM) for the J, H, and K bands, respectively. The Strehl ratios are ~ 0.02, 0.09, and 0.18 for the J, H, and K bands, respectively.

4. Results and Discussion

4.1. Orbital Motion within the Multiple System T Tauri

T Tau Sa and Sb are well resolved in the K band images taken on 2002 November 20 and 2004 November 23, as are shown in figures 2(a) and 2(b), respectively. The relative astrometry of T Tau N, Sa, and Sb at various observing epochs are summarized in table 1. The separation and position angle for the T Tau N and T Tau Sa pair agree well with those of $0{.}''691 \pm 0{.}''018$ and $182° \pm 1°$ measured on 2002 December 24 (Furlan et al. 2003).

Figure 3 shows the positions of T Tau Sb with respect to T Tau Sa at various observing epochs, confirming that our astrometry is consistent with those of the previous high-resolution near-infrared observations. The position of T Tau Sb is, however, inconsistent with the track of the southern compact radio component T Tau Sc. Our observations, including the 2004 data, support the conclusion of Furlan et al. (2003) that T Tau Sb is in a bound orbit around T Tau Sa and that it is not the radio source.

4.2. Time Variability in T Tau S (Sa and Sb)

We performed point spread function fitting using reference star images, examined the flux of T Tau Sa and Sb individually for each frame observed on 2002 November 20, and averaged the measurements for all the frames to obtain the flux. The error is the standard deviation of the flux fluctuation in all the frames we obtained during our observations. In the K band, the derived flux of T Tau Sa, Sb, and the combined T Tau S binary system (Sa + Sb) on 2002 November 20 were 8.79 ± 0.10 mag, 8.55 ± 0.10 mag, and 7.91 ± 0.10 mag, respectively. In the H band, we detected only one component of T Tau S. As the separation and position angle of the companion at H are same as T Tau Sb at K, we identified the companion at H as T Tau Sb. T Tau Sa was not detected in the H band, and its detection limit was examined as $H > 11$ mag [ΔH(Sb $-$ Sa) < -1.2]. Furthermore, the $H - K$ color of T Tau Sa was constrained ($H - K > 2.2$). We then examined the flux of T Tau Sb in the H band ($H = 9.8$). We also derived the $H - K$
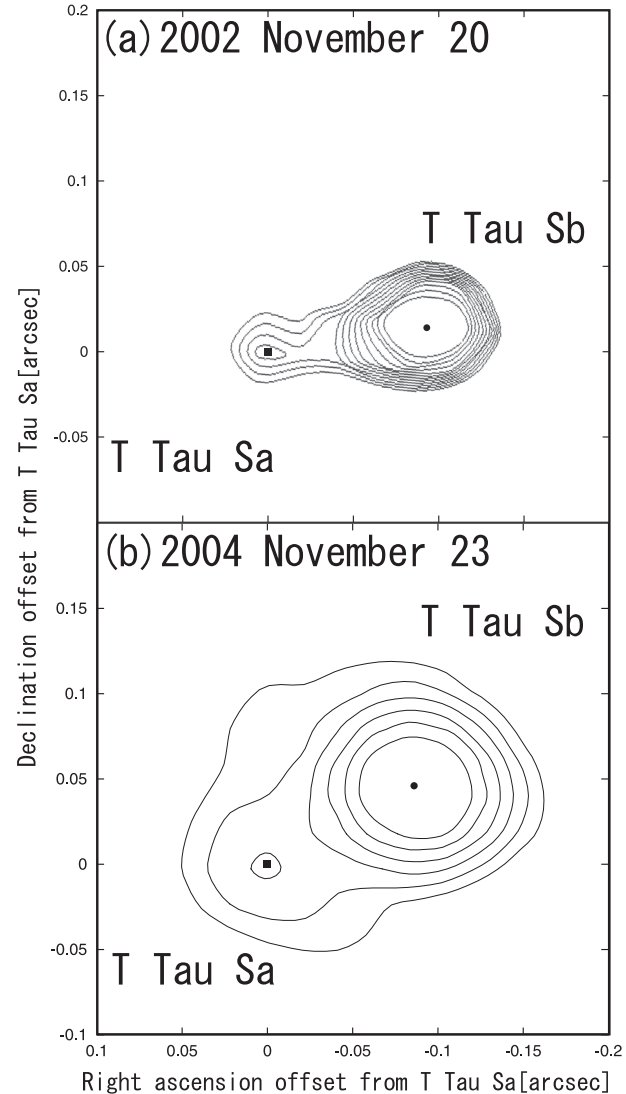

Fig. 2. K band contour map of T Tau Sa and Sb. The image was produced before subtraction of a PSF image. North is up and east toward the left. FOV is $0{.}''3$. The filled square and the filled circle are T Tau Sa and Sb, respectively. The peak positions were measured with IMEXAMINE task in IRAF. (a) T Tau Sa and Sb in 2002. The contour is logarithmic starting from the highest level of 4.6 Jy arcsec^{-2}, and spaced with a factor of $10^{-0.008}$ between successive levels. (b) T Tau Sa and Sb in 2004. The contour is logarithmic starting from the highest level of 3.8 Jy arcsec^{-2}, and spaced with a factor of $10^{-0.05}$ between successive levels.

color of T Tau Sb as ($H - K = 1.3$ mag). The redder color of T Tau Sa compared to T Tau Sb suggests that it is more deeply embedded.

Because neither a photometric standard star nor PSF reference stars were observed on 2004 November 23, we derived the fluxes of T Tau Sa and T Tau Sb with respect to T Tau N, which we assumed to have the same flux as it did on 2002 December 24 (Furlan et al. 2003). The K band flux of T Tau N did not show more than 0.2 mag of variation during the 8 yr of monitoring by Beck et al. (2004), so this assumption is plausible. The K band fluxes of T Tau Sa, Sb, and the combined T Tau S binary system (Sa + Sb) were
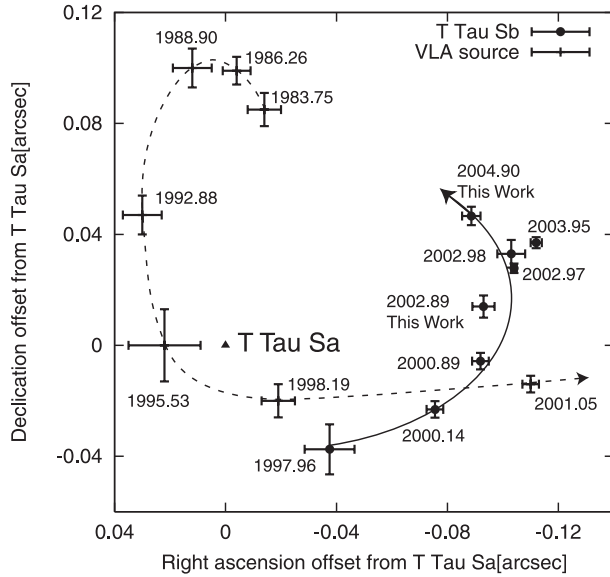
Fig. 3. Motions of T Tau Sb and VLA source with respect to T Tau Sa. The number gives the epoch of the observation. The presented data are from Koresko (2000), Köhler, Kasper, and Herbst (2000), Duchêne, Ghez, and McCabe (2002), Loinard, Rodríguez, and Rodríguez (2003), Furlan et al. (2003), Beck et al. (2004), Duchêne et al. (2005), and this work.
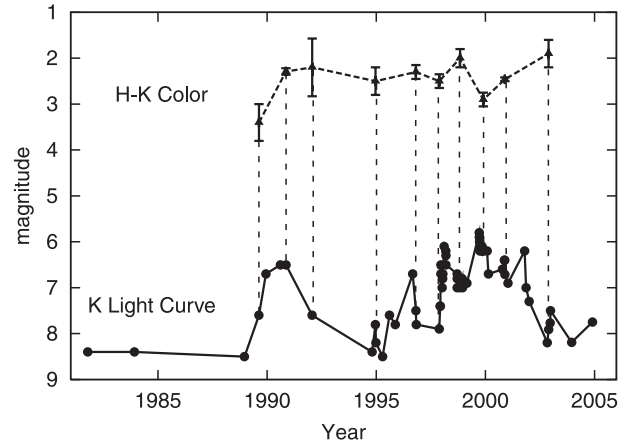

Fig. 4. Light curve in the K band and the $H - K$ color curve of T Tau S. The typical uncertainties in the magnitudes are about ± 0.1. The dashed lines connect the data points of the same epoch between the K light curve and $H - K$ color. The presented data are from this work, Dyck, Simon, and Zuckerman (1982), Beckwith et al. (1984), Maihara and Kataza (1991), Ghez et al. (1991), Tessier, Bouvier, and Lacombe (1994), Kobayashi et al. (1994), Simon et al. (1996), Roddier et al. (2000), Herbst, Robberto, and Beckwith (1997), White and Ghez (2001), Koresko (2000), Kasper et al. (2002), Duchêne, Ghez, and McCabe (2002), Furlan et al. (2003), Beck et al. (2004), and Duchêne et al. (2005).

(8.85 ± 0.42) mag, (8.25 ± 0.44) mag, and (7.75 ± 0.34) mag on 2004 November 23, respectively. Table 2 lists the cumulative results of observations that resolved T Tau Sa–Sb at K.

The time variation of the K band flux and $H - K$ color in T Tau S (Sa + Sb) since 1982 are plotted in figure 4. Figure 5(b) shows the individual fluxes of T Tau Sa and Sb since their

first resolved observation in 1997, and figure 5(a) shows the fluxes of T Tau S during a same epoch as figure 5(b). Our measurements added data points for the two recent epochs, showing that the K band flux did not undergo a significant increase of more than 0.8 mag since 2002, before which it had been ~ 1.5 mag brighter for the 4 yr. Examining the individual

Table 1. Relative astrometry of T Tau N, Sa, and Sb.

| Date (UT)	Separation [arcsec]	PA [deg]	Reference
Sb–Sa			
1997 Dec 15	0.053 ± 0.009	225 ± 8	(Koresko 2000)
2000 Feb 20	0.079 ± 0.002	253 ± 2	(Köhler et al. 2000)
2000 Nov 19	0.092 ± 0.003	267 ± 1.6	(Duchêne et al. 2002)
2002 Oct 30	0.107 ± 0.004	283.4 ± 2.1	(Beck et al. 2004)
2002 Nov 20	0.0943 ± 0.0033	278 ± 1	This work
2002 Dec 13	0.108 ± 0.001	284.9 ± 0.9	(Duchêne et al. 2005)
2002 Dec 20	0.110 ± 0.004	282.0 ± 2.1	(Beck et al. 2004)
2002 Dec 24	0.107 ± 0.005	289 ± 1	(Furlan et al. 2003)
2003 Dec 12	0.118 ± 0.002	288.6 ± 1.1	(Duchêne et al. 2005)
2004 Nov 23	0.100 ± 0.002	298 ± 1	This work
Sa–N			
2000 Nov 19	0.702 ± 0.005	179.7 ± 0.2	(Duchêne et al. 2002)
2002 Oct 20	0.697 ± 0.002	183.1 ± 0.3	(Beck et al. 2004)
2002 Nov 20	0.693 ± 0.004	183 ± 1	This work
2002 Dec 13	0.695 ± 0.007	183.3 ± 0.7	(Duchêne et al. 2005)
2002 Dec 24	0.691 ± 0.002	181.7 ± 0.4	(Furlan et al. 2003)
2003 Dec 12	0.698 ± 0.005	181.9 ± 1.2	(Duchêne et al. 2005)
2004 Nov 23	0.690 ± 0.003	186 ± 1	This work
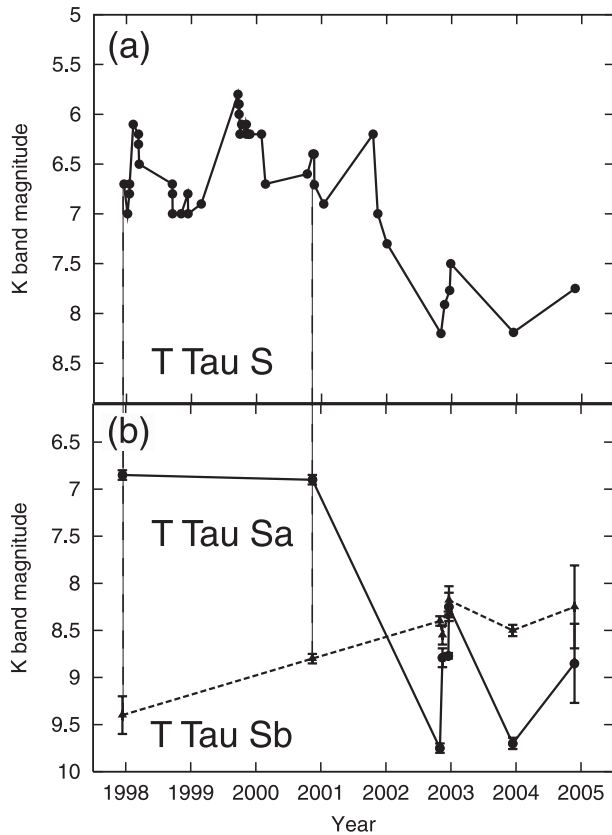
Fig. 5. (a) Light curves of T Tau S. The typical uncertainties in the magnitude are about ±0.1. (b) Light curves of T Tau Sa and Sb. The dashed lines connect the data points of the same epoch between 5(a) and 5(b). The presented data are from Koresko (2000), Duchêne, Ghez, and McCabe (2002), Furlan et al. (2003), Beck et al. (2004), Duchêne et al. (2005), and this work.

Fig. 6. *JHK* color-composite CIAO image of T Tau. The field of view is $8'' \times 9''$. North is up and east toward the left.

flux variations of T Tau Sa and Sb in figure 5(b), we found that T Tau Sb shows neither as large nor as rapid variation as T Tau Sa. While T Tau Sa dominates the flux of T Tau S rather than T Tau Sb from 1997 December to 2000 November, flux of T Tau Sa showed a significant decrease by 2.85 mag in 2002 November and T Tau Sb had begun dominating the flux of the T Tau S system. After that the flux of T Tau Sb has shown a constant level, and has still been dominating the flux of T Tau S since 2002 November. Our measurements are consistent with this tendency, which was pointed out by Duchêne et al. (2005), who proposed that T Tau Sa dominated the flux
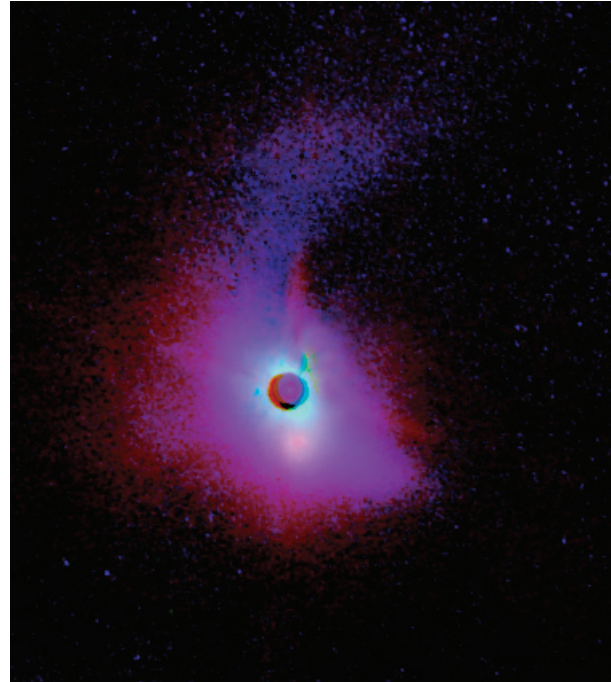
of T Tau S and accordingly the strong historic variability, as shown in figure 5(a).

The cause of the flux variation of T Tau S, presumably dominated by T Tau Sa, has been considered since the rapid increase of 2 mag in 1989 was detected by Ghez et al. (1991), who suggested that the flare may have been caused by an increase in accretion because the spectral energy distributions both before and after the flare are fit by an accretion disk model similar to those that explain FU Ori outbursts (Hartmann, Kenyon 1985). Beck et al. (2004) compiled the K and L' flux measurements of T Tau S, and found that the $K - L'$ color is correlated with the K band flux in a manner consistent with the interstellar extinction law, suggesting that obscuration is a dominant cause of the flux variation, although other processes also play a role.

Recent high-resolution near-infrared spectroscopy has detected the CO absorption lines from warm (~ 390 K) and dynamically stable ($\Delta V < 4$ km s^{-1}) gas exclusively toward T Tau Sa (Duchêne et al. 2005). This result strongly supports

Table 2. Fluxes of T Tau S, Sa, and Sb in the K band.

Date (UT)	S [Jy]	Sa [Jy]	Sb [Jy]	Reference
1997 Dec 15	1.14	1.04	0.10	(Koresko 2000)
2000 Nov 19	1.36 ± 0.05	1.15 ± 0.07	0.20 ± 0.02	(Duchêne et al. 2002)
2002 Oct 30	0.35	0.08	0.27	(Beck et al. 2004)
2002 Nov 20	0.45 ± 0.03	0.20 ± 0.02	0.25 ± 0.02	This work
2002 Dec 13	0.51 ± 0.01	0.204 ± 0.006	0.306 ± 0.008	(Duchêne et al. 2005)
2002 Dec 24	0.66 ± 0.14	0.33 ± 0.07	0.35 ± 0.07	(Furlan et al. 2003)
2003 Dec 12	0.35 ± 0.02	0.087 ± 0.006	0.262 ± 0.014	(Duchêne et al. 2005)
2004 Nov 23	0.52 ± 0.14	0.19 ± 0.09	0.33 ± 0.11	This work

the presence of a few AU size edge-on disk, which would be asymmetric and responsible for the observed time variation of T Tau Sa.

It nonetheless seems inappropriate to attribute all of the time variability to a time variable absorber, because not all of the changes are consistent with a simple reddening law. For example, the flare observed by Ghez et al. (1991) did not show any color variation in the near- to mid-infrared wavelengths. Also, the $H - K$ color appeared redder from 2.0 mag to 2.9 mag, while the K band magnitude had become brighter from 7.0 mag to 6.2 from 1998 November to 1999 November (Roddier et al. 2000). Moreover, during one event the $H - K$ color became bluer when the K-band flux decreased. The $H - K$ color was (1.9 ± 0.3) mag with a K flux of 7.9 mag on 2002 November 20, while it was (2.5 ± 0.1) mag with a K flux of 6.7 mag on 2000 November 19 (Duchêne et al. 2002). A change in the accretion rate may be the dominant cause for such events, as suggested by the strong correlation between the Brγ emission and the near-infrared flux.

4.3. Nebulosity

Details of the faint near-infrared nebulosity have for the first time emerged at subarcsec resolutions, thanks to coronagraphic observations. The arc-like ridge extending to the north and to the southwest through T Tau N in the near-infrared images is consistent with that in the optical one (figure 1), supporting the interpretation that the arc is part of the cavity wall seen relatively pole-on (Momose et al. 1996; Stapelfeldt et al. 1988). The northern ridge is $4''$ long and the southwestern ridge is $\sim 2''.5$ long.

Besides the arc, the near-infrared images show significant halo emission around T Tau N, even after its PSF has been subtracted, while no halo emission around T Tau N is seen in the optical image. Figure 6 shows the *JHK* color-composite image. The nebula appears to become more circular and more diffuse with increasing wavelengths. At longer wavelengths, we are seeing more diffuse and much redder region in contrast with the image at shorter wavelengths. The color-composite image indicates that T Tau nebula consists of two different structures, which are redder halo emission and a bluer arc-like ridge. The halo emission was detected within $\sim 2''.5$ from T Tau N, slightly elongated along the PA = 45°. This length scale is much larger than that of the submillimeter disk emission (FWHM $\sim 0''.4$), which was detected toward T Tau N, but not toward T Tau S (Hogerheijde et al. 1997; Akeson et al. 1998). It is, however, comparable to the size of the HCO$^+$

emission ($\sim 2''$) surrounding both T Tau N and S (Hogerheijde et al. 1997) and that of the envelope (FWHM $\sim$ several arcsec) detected in the submillimeter thermal emission (Weintraub et al. 1999). It is thus natural to suggest that the halo emission is the near-infrared light scattered by the common envelope surrounding the T Tauri multiple system, rather than by disk around T Tau N or around the multiple system.

5. Summary

We have conducted *JHK* band adaptive optics coronagraphic observations of the enigmatic T Tau multiple system. The main conclusions are as follows:

1. The infrared companion close pair T Tau Sa and Sb is resolved in the K band. The curvature and orientation of the path of T Tau Sb probably indicate that it is bound to T Tau Sa, as has been inferred by Furlan et al. (2003).
2. The flux of T Tau S at the time of our observations (2002 November 23) obviously decreased in the K band by about 1.7 Jy from its maximum value, which was observed in 2001 (Beck et al. 2004). This is probably caused by both a variation in the accretion rate and variable extinction.
3. While the K-band flux of T Tau Sa was larger than that of Sb in 2000 November (Sa/Sb = 5.7, Duchêne et al. 2002), the flux of T Tau Sb was larger than that of Sa at the time of our observation (Sa/Sb = 0.79, 2002 November and Sa/Sb = 0.58, 2004 November). The flux decrease of the whole T Tau S system from 2000 to 2002 was mainly caused by T Tau Sa.
4. Halo emission was detected out to $\sim 2''$ from T Tau N. This can be scattered near-infrared light off the common envelope surrounding the T Tauri multiple system.

References

Akeson, R. L., Koerner, D. W., & Jensen, E. L. N. 1998, ApJ, 505, 358

Beck, T. L., Prato, L., & Simon, M. 2001, ApJ, 551, 1031

Beck, T. L., Schaefer, G. H., Simon, M., Prato, L., Stoesz, J. A., & Howell, R. R. 2004, ApJ, 614, 235

Beckwith, S., Zuckerman, B., Skrutskie, M. F., & Dyck, H. M. 1984, ApJ, 287, 793

Bertout, C., Basri, G., & Bouvier, J. 1988, ApJ, 330, 350

Duchêne, G., Ghez, A. M., & McCabe, C. 2002, ApJ, 568, 771

Duchêne, G., Ghez, A. M., McCabe, C., & Ceccarelli, C. 2005, ApJ, 628, 832

Dyck, H. M., Simon, T., & Zuckerman, B. 1982, ApJ, 255, L103

Elias, J. H. 1978, ApJ, 224, 857

Furlan, E., Forrest, W. J., Watson, D. M., Uchida, K. I., Brandl, B. R., Keller, L. D., & Herter, T. L. 2003, ApJ, 596, L87

Ghez, A. M., Neugebauer, G., Gorham, P. W., Haniff, C. A., Kulkarni, S. R., Matthews, K., Koresko, C., & Beckwith, S. 1991, AJ, 102, 2066

Hartmann, L., & Kenyon, S. J. 1985, ApJ, 299, 462

Herbst, T. M., Robberto, M., & Beckwith, S. V. W. 1997, AJ, 114, 744

Hogerheijde, M. R., van Langevelde, H. J., Mundy, L. G., Blake, G. A., & van Dishoeck, E. F. 1997, ApJ, 490, L99

Johnston, K. J., Gaume, R. A., Fey, A. L., De Vegt, C., & Claussen, M. J. 2003, AJ, 125, 858

Joy, A. H. 1945, ApJ, 102, 168

Kasper, M. E., Feldt, M., Herbst, T. M., Hippler, S., Ott, T., & Tacconi-Garman, L. E. 2002, ApJ, 568, 267

Kobayashi, N., Nagata, T., Hodapp, K.-W., & Hora, J. L. 1994, PASJ, 46, L183

Köhler, R., Kasper, M., & Herbst, T. 2000, in Birth and Evolution of Binary Stars, ed. B. Reipurth & H. Zinnecker (San Francisco: ASP), 63

Koresko, C. D. 2000, ApJ, 531, L147

Koresko, C. D., Herbst, T.M., & Leinert, Ch. 1997, ApJ, 480, 741

Loinard, L., Rodríguez, L. F., & Rodríguez, M. I. 2003, ApJ, 587, L47

Maihara, T., & Kataza, H. 1991, A&A, 249, 392

Momose, M., Ohashi, N., Kawabe, R., Hayashi, M., & Nakano, T. 1996, ApJ, 470, 1001

Nakajima, T., & Golimowski, D. A. 1995, AJ, 109, 1181

Robberto, M., Clampin, M., Ligori, S., Paresce, F., Sacca, V., & Staude, H. J. 1995, A&A, 296, 431

Roddier, F., Roddier, C., Brandner, W., Charissoux, D., Véran, J.-P., & Courbin, F. 2000, in Birth and Evolution of Binary Stars, ed. B. Reipurth & H. Zinnecker (San Francisco: ASP), 60

Schwartz, P. R., Simon, T., & Campbell, R. 1986, ApJ, 303, 233

Simon, M., Close, L. M., & Beck, T. L. 1999, AJ, 117, 1375

Simon, M., Longmore, A. J., Shure, M. A., & Smillie, A. 1996, ApJ, 456, L41

Smith, K., Pestalozzi, M., Güdel, M., Conway, J., & Benz, A. O. 2003, A&A, 406, 957

Stapelfeldt, K. R., et al. 1998, ApJ, 508, 736

Takami, H., et al. 2004, PASJ, 56, 225

Tamazian, V. S. 2004, AJ, 127, 2378

Tamura, M., et al. 2000, Proc. SPIE, 4008, 1153

Tessier, E., Bouvier, J., & Lacombe, F. 1994, A&A, 283, 827

Weintraub, D. A., Kastner, J. H., Zuckerman, B., & Gatley, I. 1992, ApJ, 391, 784

Weintraub, D. A., Sandell, G., Huard, T. L., Kastner, J. H., van den Ancker, M. E., & Waters, R. 1999, ApJ, 517, 819

White, R. J., & Ghez, A. M. 2001, ApJ, 556, 265